Supplemental Dataset 1: Plots of all genes dendritically enriched in Slide-seqV2

Supplemental Dataset 2: Plots of all genes called as Spatially Significant in Slide-seqV2

Supplementary Table 1: Sequencing and alignment metrics across Slide-seq conditions.

Condition	# Unique UMIs in first 10k barcodes	% Mapping	% Genic
Chemgenes beads, Dibase (Slide-seqV1)	2,190,749	61.5%	83.7%
Second Strand Synthesis, Chemgenes beads, Dibase	10,218,631	84.8%	85.4%
Second Strand Synthesis, Chemgenes beads, Monobase	8,930,245	79.9%	83.6%
Second Strand Synthesis, Custom beads, Monobase (Slide-seqV2)	19,563,646	80.8%	82.5%

% Mapping is the percentage of Illumina reads which map to the genomic reference.
% Genic is the percentage of mapped reads which align to genic regions.

Supplementary Table 2: Mean and Standard Deviation of Gene Measurements Fig. 1D (total over 200 cells).

	smFISH	scRNAseq	Slide-seq	Slide-seqV2
Atp2b1	17758∓3882	6700∓225	133∓17	3131∓73
Ociad2	8681∓1496	424∓22	53.5∓6	444∓17
Slc17a7	8477∓617	246∓9	21.5∓3	383∓12

Supplementary Table 3: Dendritically enriched gene-sets.

Sheet 1: Dendritically enriched RNAs identified by Slide-seqV2 along with Fold-Change enrichment, and FDR corrected q-value.

Sheet 2: Differentially expressed genes between CA1 and other scRNA-seq clusters which were removed from the dendritic analysis.

Sheet 3: Grouping of dendritically enriched genes by spatial clusters.

Sheet 4: List of genes which overlap with Tushev et al., 2018, and Ainsley et al., 2016 as well as genes uniquely identified by Slide-seqV2.

Supplementary Table 4: List of all genes called as Spatially Significant for Slide-seqV2 data in the developing cortex (Sheet 1) and eye (Sheet 2)

Supplementary Table 5: List of genes unique to each method regarding the trajectory inference:

Sheet 1: Genes unique to Slide-seqV2
Sheet 2: Genes unique to monocle3
Sheet 3: Genes unique to scVelo

Supplementary Table 6: Oligonucleotide sequences used in the study.

Name	Sequence
Template Switch Oligo	AAGCAGTGGTATCAACGCAGAGTGAATrG+GrG
Truseq_PCR_Handle	CTACACGACGCTCTTCCGATCT
SMART_PCR_Primer	AAGCAGTGGTATCAACGCAGAGT
dN-SMRT oligo	AAGCAGTGGTATCAACGCAGAGTGANNNGGNNNB
Truseq P5	AATGATACGGCGACCACCGAGATCTACACTCTTTCCCTACACGACGC TCTTCCGATCT
Truseq-1	/5phos/GATCGGAAGAGCGTCGTGTAG
Truseq	/5phos/AGATCGGAAGAGCGTCGTGTAG
Truseq+1	/5phos/NAGATCGGAAGAGCGTCGTGTAG
Truseq+2	/5phos/NNAGATCGGAAGAGCGTCGTGTAG
Truseq(8b)+3	/5phos/NNNAGATCGGA/3InvdT/
3UP-1	TCTCGGGAACGCTGAAG
3UP	TCTCGGGAACGCTGAAGA
3UP+1	TCTCGGGAACGCTGAAGAN
UP-1	/5phos/CTCGGGAACGCTGAAGA
UP	/5phos/TCTCGGGAACGCTGAAGA
UP+1	/5phos/NTCTCGGGAACGCTGAAGA
UP+2	/5phos/NNTCTCGGGAACGCTGAAGA

UP(7b)+3	/5phos/NNNTCTCGGG/3InvdT/
UP(7b)+4	/5phos/NNNNTCTCGGG/3InvdT/
Monobase 5A	/6FAM/IIINNNAN
Monobase 5G	/aquaphluor593/IIINNNGN
Monobase 5C	/CY3/IIINNNCN
Monobase 5T	/Cy5/IIINNNTN
Monobase 3A	/5Phos/NANNNIII/6FAM/
Monobase 3G	/5Phos/NGNNNIII/aquaphluor593/
Monobase 3C	/5Phos/NCNNNIII/Cy3/
Monobase 3T	/5Phos/NTNNNIII/Cy5/

Supplementary Table 7: Puck metadata associated with each experiment, all arrays Slide-seqV2 library preparation unless otherwise noted

Figure	Puck Used (Tissue Type)
1A	Puck_200115_08 (mouse hippocampus)
1B	Puck_190926_03 (mouse embryo) Puck 191007_07 (mouse embryo Slide-seq)
1C/D	Puck_200115_08 (mouse hippocampus)
2	Puck_191204_01 (mouse hippocampus) Puck_191219_17 (mouse hippocampus) Puck_191219_18 (mouse hippocampus) Puck_191219_20 (mouse hippocampus)
3	Puck_190921_19* (mouse E15 brain)
S3	Puck_200115_08 (mouse hippocampus), visium data is coronal section from 10x website Puck_200127_15 (mouse olfactory bulb), HDST data is from published data
S4	Puck_200306_03 (mouse somatosensory cortex)
S5	Puck_200115_08 (S5A-B, mouse hippocampus) Puck_200306_03, Puck_200306_02 (S5C, mouse somatosensory cortex)
S6	Puck_191204_01 (mouse hippocampus) Puck_191219_17 (mouse hippocampus) Puck_191219_18 (mouse hippocampus) Puck_191219_20 (mouse hippocampus)
S7	Puck_190921_19* (mouse E15 brain) Puck_190926_03 (E12.5 mouse embryo)
S8	Puck_190921_19* (mouse E15 brain) Puck_190926_03 (E12.5 mouse embryo)

Supplementary Table 7	Puck_190926_01, Puck_190926_02, Puck_190926_03, Puck_190926_06

* denotes use of original dibase indexing scheme

Supplementary Table 8: Running time of the Slide-seq tools pipeline.

Steps	# libraries	# lanes	# slices	Parallel	Size of bam	# barcodes	Time (minutes)
Extract Illumina barcodes	4	1	10	Per lane			44
Convert Illumina basecalls to bam	4	1	1	Per slice	600M		25
Align reads	1	1	1	Per slice	600M		35
Merge and validate bam	1	2	10		10G		60
Select cells by the number of transcripts	1	2	10		10G	300K	50
Generate alignment reports and plots	1	2	10		10G		70
Barcode matching	1	2	10	Per 100K barcodes		100K vs 85K	30
Generate digital expression and plots for matched barcodes	1	2	10		4G	50K	110

Supplementary Figures:

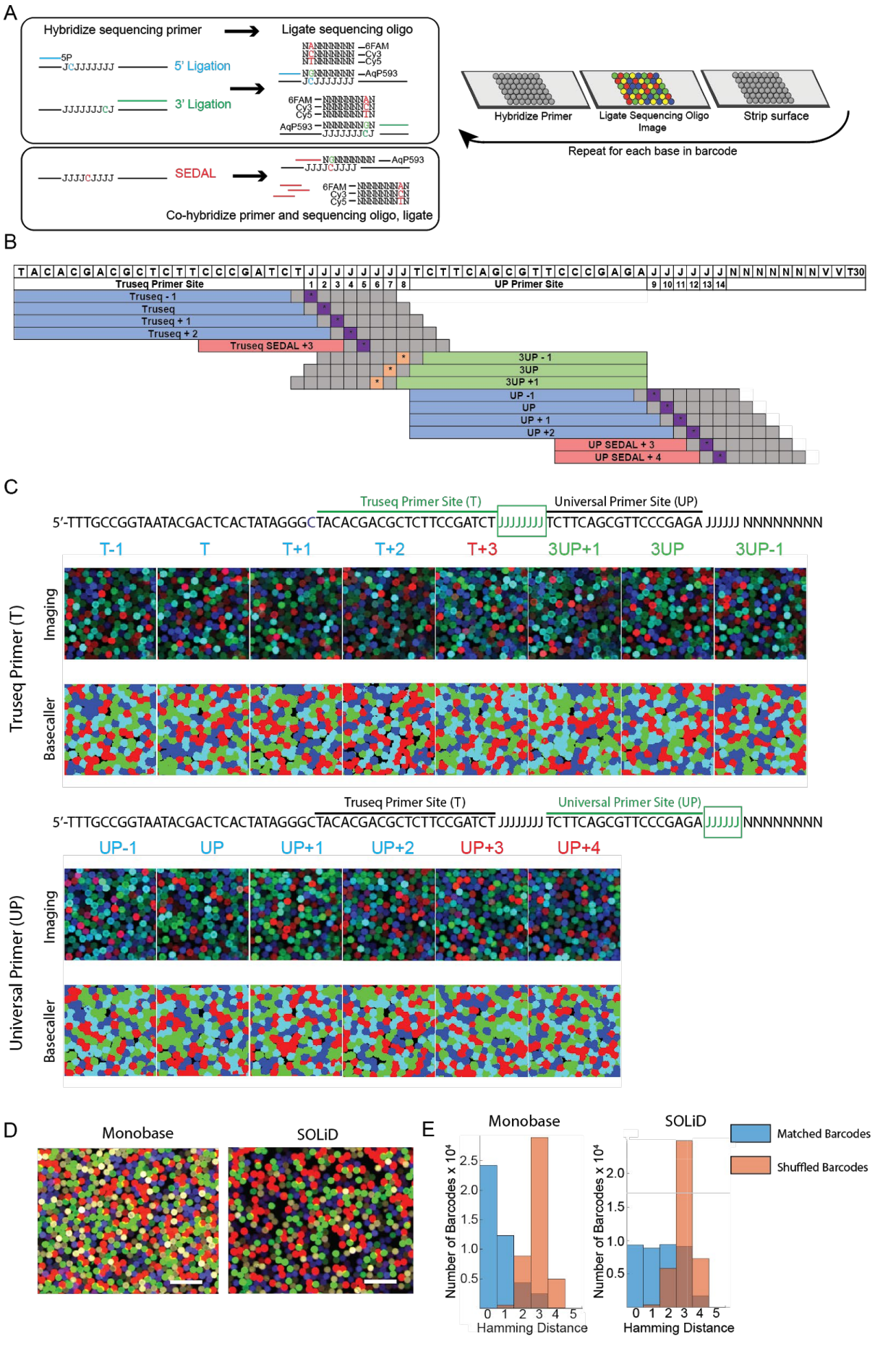
A
Hybridize sequencing primer
Ligate sequencing oligo
5' Ligation
3' Ligation
SEDAL
Co-hybridize primer and sequencing oligo, ligate
Hybridize Primer
Ligate Sequencing Oligo
Strip surface
Image
Repeat for each base in barcode
B
Truseq Primer Site
UP Primer Site
Truseq - 1
Truseq
Truseq + 1
Truseq + 2
Truseq SEDAL +3
3UP - 1
3UP
3UP +1
UP -1
UP
UP + 1
UP +2
UP SEDAL + 3
UP SEDAL + 4
C
Truseq Primer Site (T)
Universal Primer Site (UP)
5'-TTTGCCGGTAATACGACTCACTATAGGGCTACACGACGCTCTTCCGATCT JJJJJJJJ TCTTCAGCGTTCCCGAGA JJJJJJ NNNNNNNN
T-1
T
T+1
T+2
T+3
3UP+1
3UP
3UP-1
Truseq Primer (T)
Imaging
Basecaller
UP-1
UP
UP+1
UP+2
UP+3
UP+4
Universal Primer (UP)
D
Monobase
SOLiD
E
Monobase
SOLiD
Matched Barcodes
Shuffled Barcodes
Number of Barcodes x 10⁴
Hamming Distance

Figure S1: **Monobase sequencing by ligation chemistry allows for replacement of SOLiD sequencing for array generation**.

A) Right) schematic representations of the 3 different variants of sequencing by ligation used (5' ligation, 3' ligation, and SEDAL). Note that for the monobase ligations, the fluorophore encodes the base identity at position 2 from the ligation junction. Left) Schematic for order of operations during *in situ* sequencing.

B) Each sequencing primer, and sequencing reaction, aligned against the bead sequence (top) to interrogate each of the split-pool bases (J1-14). 5' ligation primers are shown in blue, 3' ligation primers are shown in green, SEDAL primers are shown in red. Primer sequences are listed in Table S6. The bases being interrogated with the 5' ligation sequencing oligo are highlighted in purple, and bases being interrogated with the 3' ligation sequencing oligo are highlighted in orange. Gray boxes represent degenerate bases in the sequencing oligo (e.g. Is and Ns in the sequence 5Phos/NANNNIII/6FAM/).

C) Schematic representation of each base of monobase sequencing, and an example image as well as base-call for each base. Top: bases sequenced in the first block of Js using the Truseq (blue primers) as well as the 3' sequencing off of UP (green primers). The two rows of images show the composite images from the imaging (top row) and the basecaller outputs (bottom row) Bottom: bases sequenced in the second block of Js. Color of the base being sequenced represents the type of indexing performed as outlined in part A on that base. The two rows of images show the composite images from the imaging (row labeled "Imaging") and the basecaller outputs (row labeled "Basecaller").

D) Example of four- color fluorescent images for monobase (left) and dibase (right) in situ sequencing on pucks (Lookup Table (LUT) for each channel is matched between images).

E) Histogram of barcode matching (hamming distance to closest barcode) between imaging and short read sequencing data for array imaged in monobase (left) and dibase (right).

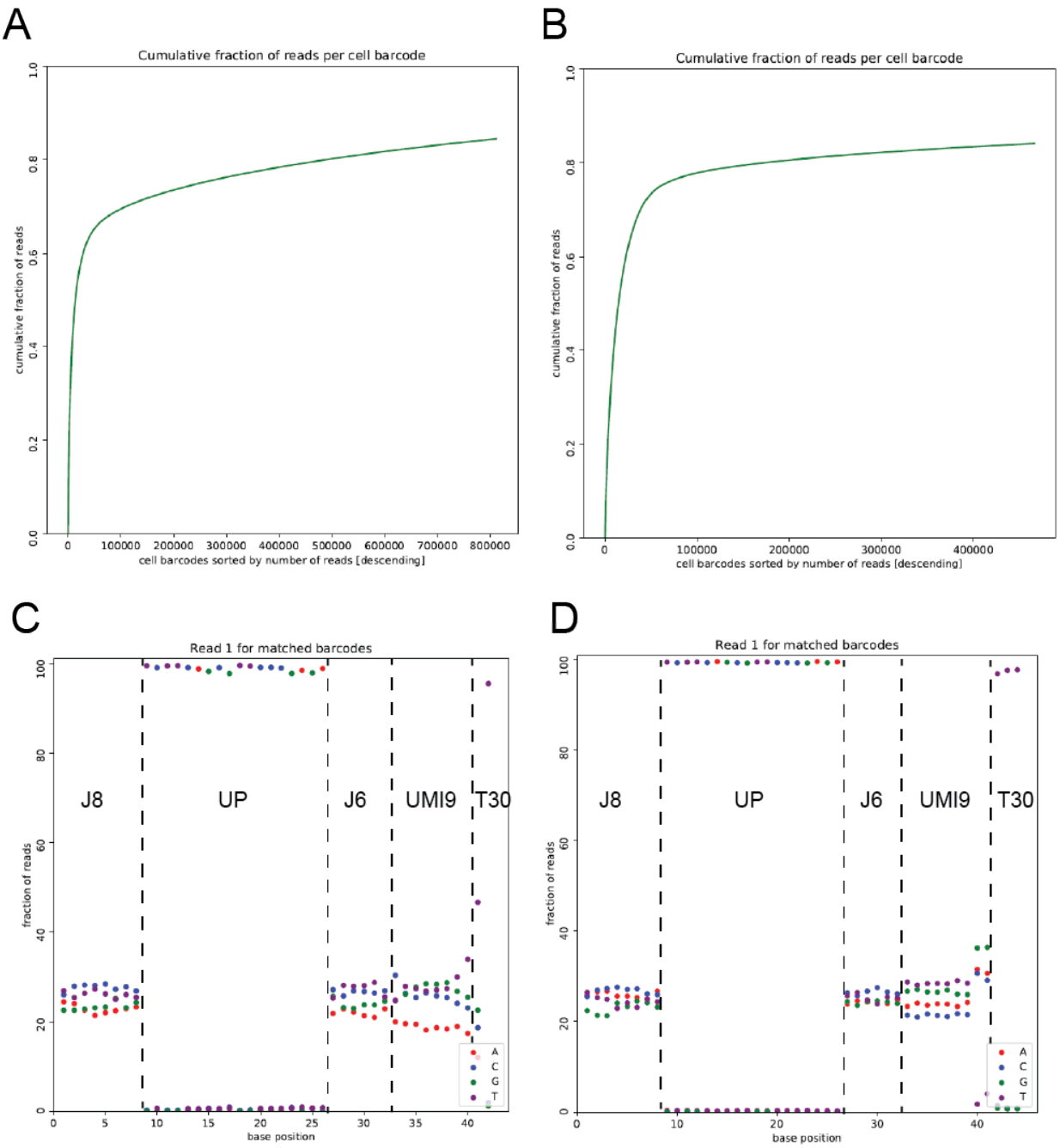

Figure S2: **Mapping and barcode matching statistics for barcoded beads used in Slide-seqV2.**

A) Cumulative distribution of reads mapping to barcodes for commercially supplied beads. There are ~100,000 beads sequenced, fraction of reads after 100,000 beads suggest synthesis errors resulting in fractured bead barcodes.

B) Cumulative distribution of reads mapping to barcodes for beads with custom optimized bead synthesis. There are ~100,000 beads sequenced, note the knee at 100,000 beads is ~80% of reads.

C) For barcodes that map to *in situ* sequenced beads, the base balance of the bead barcode for commercially supplied beads. Note the incomplete synthesis of bases in the constant bases of UP, as well as the high polyT% in the last base of the UMI, suggesting internal deletions in the bead sequence.
D) Same as C) but for custom optimized bead synthesis.

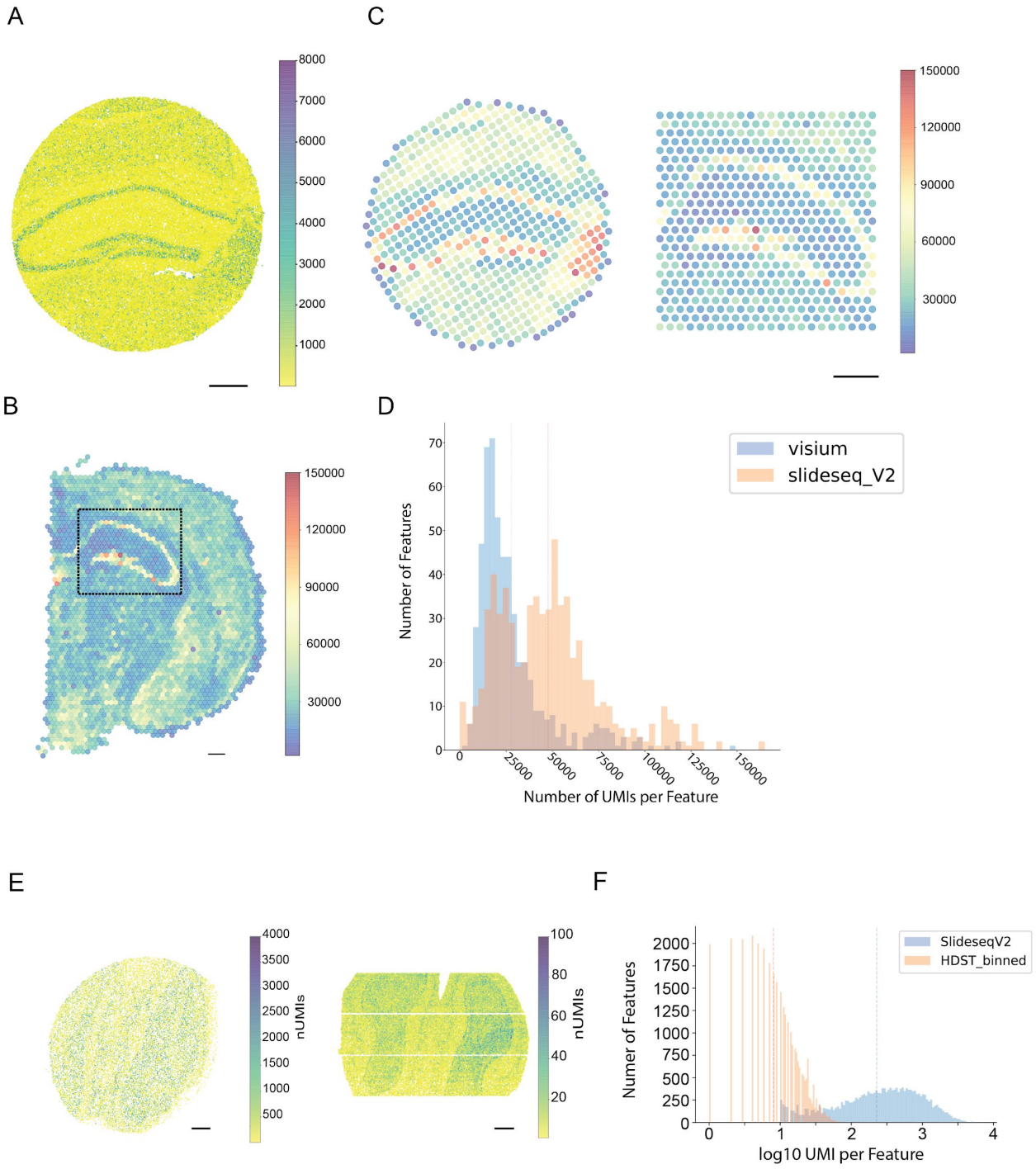

Figure S3: **Comparison of Slide-seqV2 data to existing spatial transcriptomics methods.**
A) UMI counts of a Slide-seqV2 experiment performed on the mouse hippocampus. Data displayed at 10 μm resolution.
B) Visium UMIs per feature from the mouse hippocampus. Black box indicates the cropped region used to match the cropped Slide-seqV2 region (see panel C).
C) Slide-seqV2 data (left) binned to match the feature size of the Visium data (right; each feature is 110 μm center-to-center). Scale bars represent the number of UMIs.

D) Histogram comparing number of UMIs per feature for binned Slide-seqV2 data in C and Visium data. Dotted line represents the mean of each method. (Mean binned Slide-seqV2=45,772 UMIs, Mean Visium = 27,952 UMIs)
E) Left: Slide-seqV2 of the mouse olfactory bulb. The color of each bead is defined as the number of UMIs (nUMIs). Scale bar 500 μm. Right: HDST 10 μm (5x5 binned) data of the mouse olfactory bulb. The color of each 10 μm spot is defined by the number of UMIs (nUMIs) detected.
F) Histogram of UMIs per feature for Slide-SeqV2 and HDST. Vertical dotted lines denote the mean of each dataset (11.5 UMI HDST_binned, 494UMI Slide-seqV2).
In A, B, C, and E, color-bar represents the number of UMIs.
(All scale bars 500 μm)

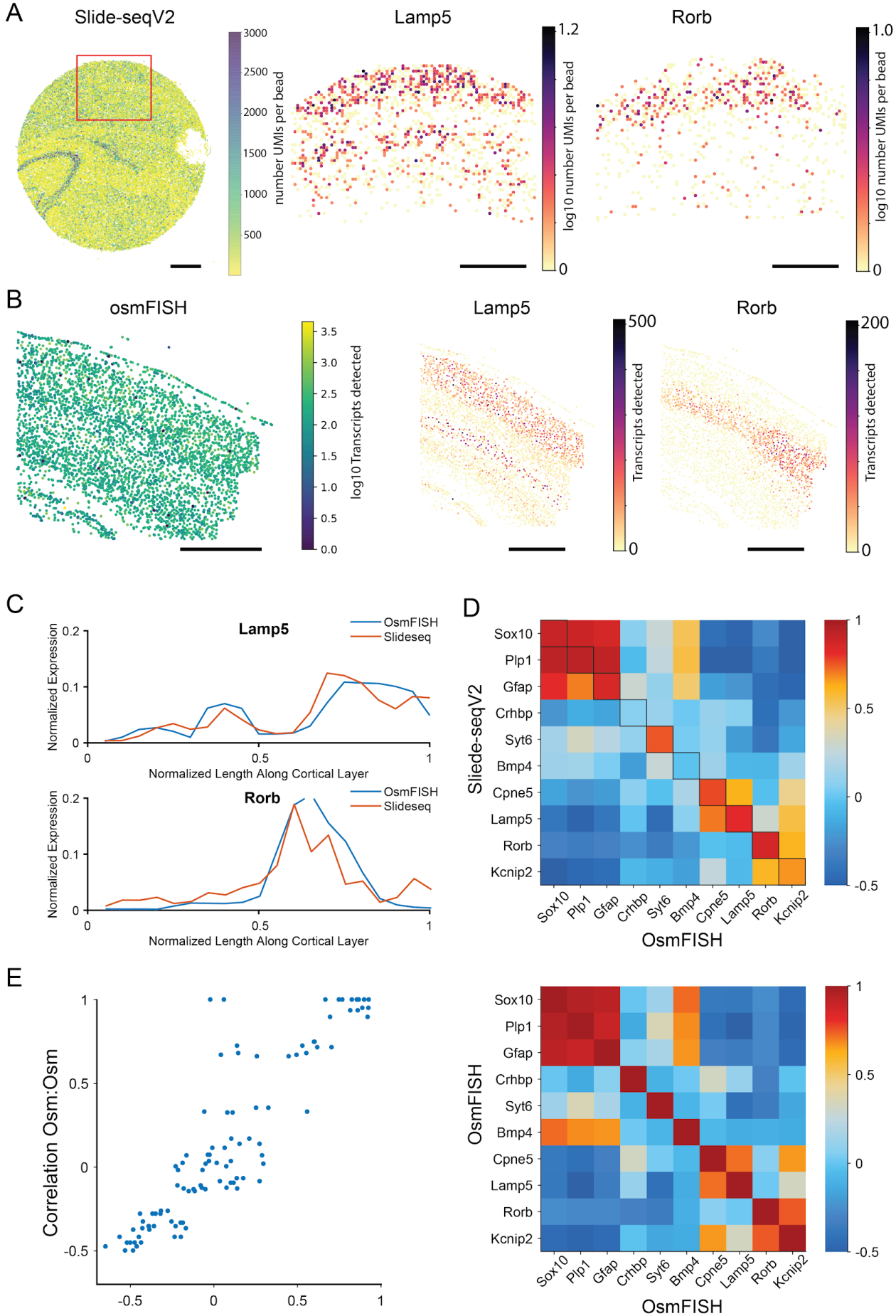
A
Slide-seqV2
number UMIs per bead
3000
2500
2000
1500
1000
500
Lamp5
log10 number UMIs per bead
1.2
0
Rorb
log10 number UMIs per bead
1.0
0
B
osmFISH
log10 Transcripts detected
3.5
3.0
2.5
2.0
1.5
1.0
0.5
0.0
Lamp5
Transcripts detected
500
0
Rorb
Transcripts detected
200
0
C
Lamp5
OsmFISH
Slideseq
Normalized Expression
0.2
0.1
0
0
0.5
1
Normalized Length Along Cortical Layer
Rorb
OsmFISH
Slideseq
Normalized Expression
0.2
0.1
0
0
0.5
1
Normalized Length Along Cortical Layer
D
Slide-seqV2
Sox10
Plp1
Gfap
Crhbp
Syt6
Bmp4
Cpne5
Lamp5
Rorb
Kcnip2
1
0.5
0
-0.5
Sox10
Plp1
Gfap
Crhbp
Syt6
Bmp4
Cpne5
Lamp5
Rorb
Kcnip2
OsmFISH
E
Correlation Osm:Osm
1
0.5
0
-0.5
-0.5
0
0.5
1
Correlation Slide-seq:Osm
OsmFISH
Sox10
Plp1
Gfap
Crhbp
Syt6
Bmp4
Cpne5
Lamp5
Rorb
Kcnip2
1
0.5
0
-0.5
Sox10
Plp1
Gfap
Crhbp
Syt6
Bmp4
Cpne5
Lamp5
Rorb
Kcnip2
OsmFISH

Figure S4: **Spatial correspondence of Slide-seqV2 to smFISH data**
A) UMIs per feature for Slide-seqV2 performed on the somatosensory cortex. Boxed region is an inset of cortex shown on the right. (Colorbar, counts) Right: Gene plots shown for two cortical markers *Lamp5*, *Rorb*. For display the beads have been binned to 20 μm by 20μm features. (Colorbar, $\log_{10}$ counts; Scale bars 500 μm)
B) Left: Counts per cell for osmFISH across 33 genes in the somatosensory cortex[1]. (Colorbar, $\log_{10}$ counts) Center: Spatial plots of *Lamp5*, *Rorb* in osmFISH. (Colorbar, counts; scale bars 500 μm)
C) Normalized expression of two cortical markers (*Lamp5*, *Rorb*) along the axis of the cortex for Slide-seq and osmFISH.
D) For each gene, the i,j^{th} entry of the heatmap is the correlation between spatial profiles between Slide-seqV2 and osmFISH (top) and osmFISH and osmFISH (bottom). Colorbar: Pearson's r.
E) Scatter plot of the pairwise Pearson's correlation of the profiles along the cortex for genes in the osmFISH dataset and Slide-seq dataset (i.e., the i,j^{th} entry of D,left against i,j^{th} entry of D, right; N=11 genes, 66 pairwise comparisons).

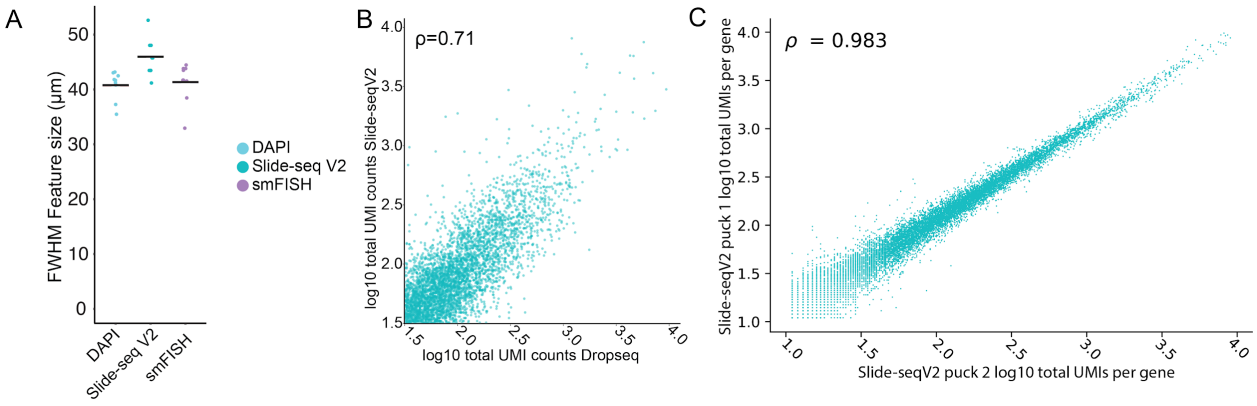

Figure S5: **Slide-seqV2 spatial diffusion, capture efficiency, and reproducibility**
A) Diffusion measurement of Slide-seqV2 by comparing the relative feature width of CA1 as compared to serial sections in both smFISH of marker genes of CA1 excitatory cells as well as DAPI. (DAPI 40.8∓2.5µm, Slide-seqV2 45∓3.1µm, smFISH Slide-seqV2 41.5∓3.4µm)
B) Measure of the relative sensitivity of Slide-seqV2 as compared to Drop-seq on a total UMI counts per gene across mouse CA1 excitatory neurons. Spearman correlation between the total UMI counts per gene of the two datasets is displayed.
C) Reproducibility of Slide-seqV2 data across two pucks processed in parallel taken as the total UMI counts per gene from the equivalent region of mouse hippocampus. Spearman correlation between the total UMI counts per gene of the two datasets is displayed.

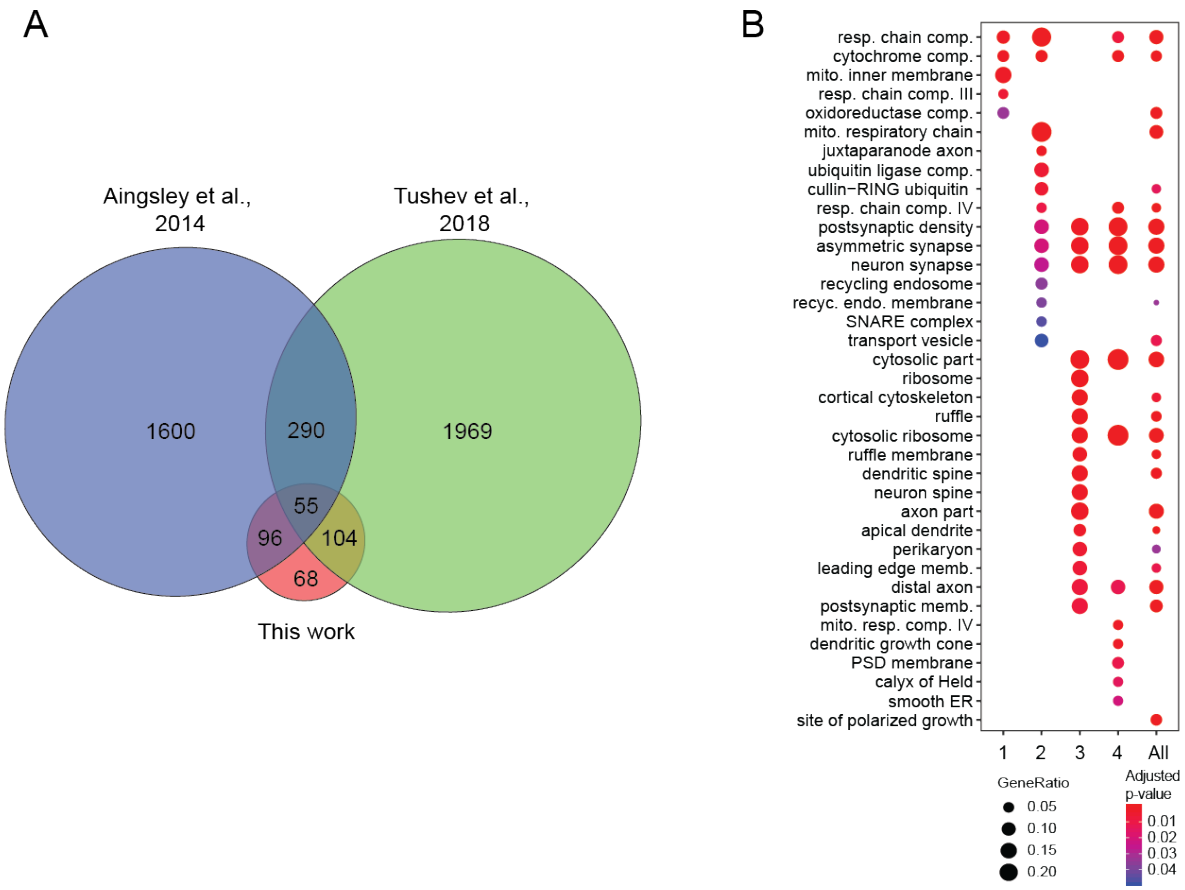

Figure S6: **Dendritically enriched RNAs identified in this work and two previous studies.** .
A) Overlap between dendritically enriched lists in this study and Aingsley et al., 2014[2], and Tushev et al., 2018[3].
B) Gene-ontology classifications using over-representation analysis (Methods) for cellular component terms for each spatial cluster in 2D as well as all dendritically enriched genes.

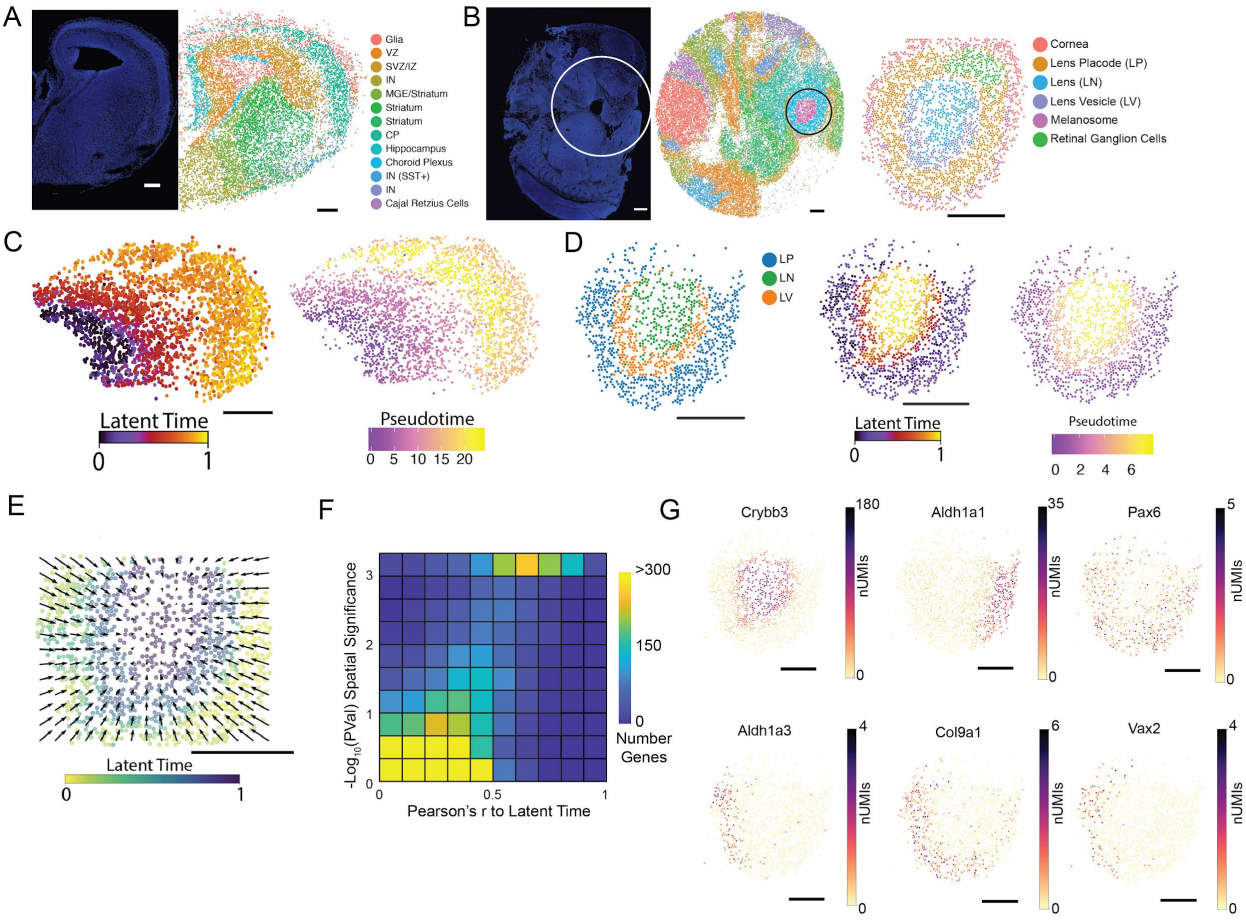

Figure S7: **Trajectory analyses of mouse E15 cortex and mouse E12.5 ocular lens.**
A) Left: DAPI stain of E15 mouse brain. This is a serial section of the region that was placed on the puck. Right: Slide-seqV2 data of E15 brain with cluster labels. VZ = Ventricular Zone, SVZ = Sub-Ventricular Zone, IZ = Intermediate Zone, IN = Interneuron, MGE = Medial Ganglionic Eminence, CP = Cortical Plate. (Scale bar 200 μm).
B) Section of E12.5 mouse embryo. Left: DAPI stained section with puck placement outlined in white line. Middle: Slide-seqV2 data of embryo section. Coloring of beads by cluster. Black circle represents the eye taken for downstream analysis. Right: Clustering of the eye with cluster labels representing different regions of the developing eye. (Scale bar 200 μm).
C) Left: Latent time trajectory generated by scVelo on expression of Slide-seqV2 for cortex data plotted in space. Right: Pseudotime generated with Monocle3 plotted in space for cotex data. (Scale bar 200 μm)
D) Left: Developing lens taken for pseudotime analysis (Blue = Lens Placode, Orange= Lens Vesicle, Green = Lens). Middle: As in C, for scVelo, but applied to the developing lens. Right: As in C, for Monocle, but applied to the developing lens. (Scale bars 200 μm).
E) Quiver plot E12.5 embryonic eye showing rate of spatial change in gene expression over the latent time axis. (Scale bar 200 μm).
F) Two-dimensional density plot quantifying the relationship between a gene's correlation with scVelo latent time (x-axis, Pearson's r) and spatial significance in embryonic eye (y-axis, log p-value, see Methods).

G) Plot of UMI counts of example genes identified as spatially significant in eye development. (Scale bar 100 μm).

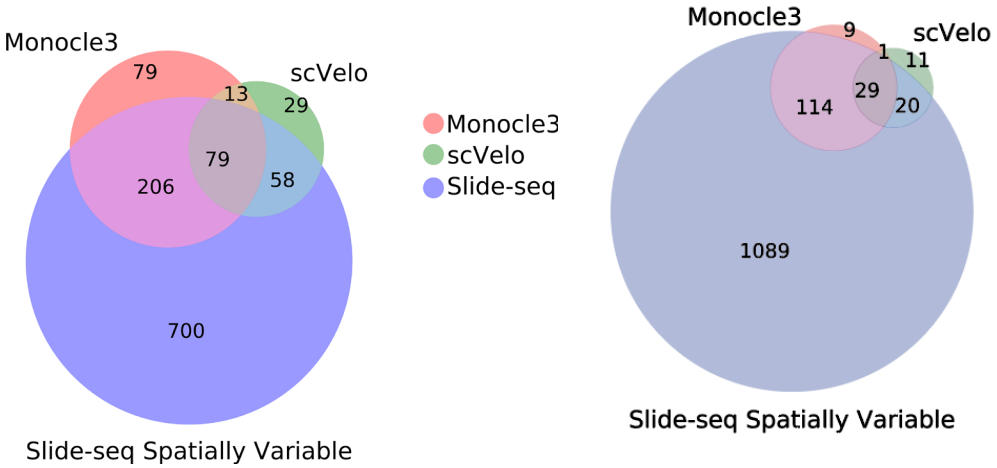

Figure S8: **Significant gene detection by trajectory inference methods versus Slide-seqV2**. Number of genes significantly loading onto Monocle3, scVelo, and the spatial developmental axis by Slide-seqV2 in E15 mouse cortex (Left) and E12.5 embryonic eye (right).

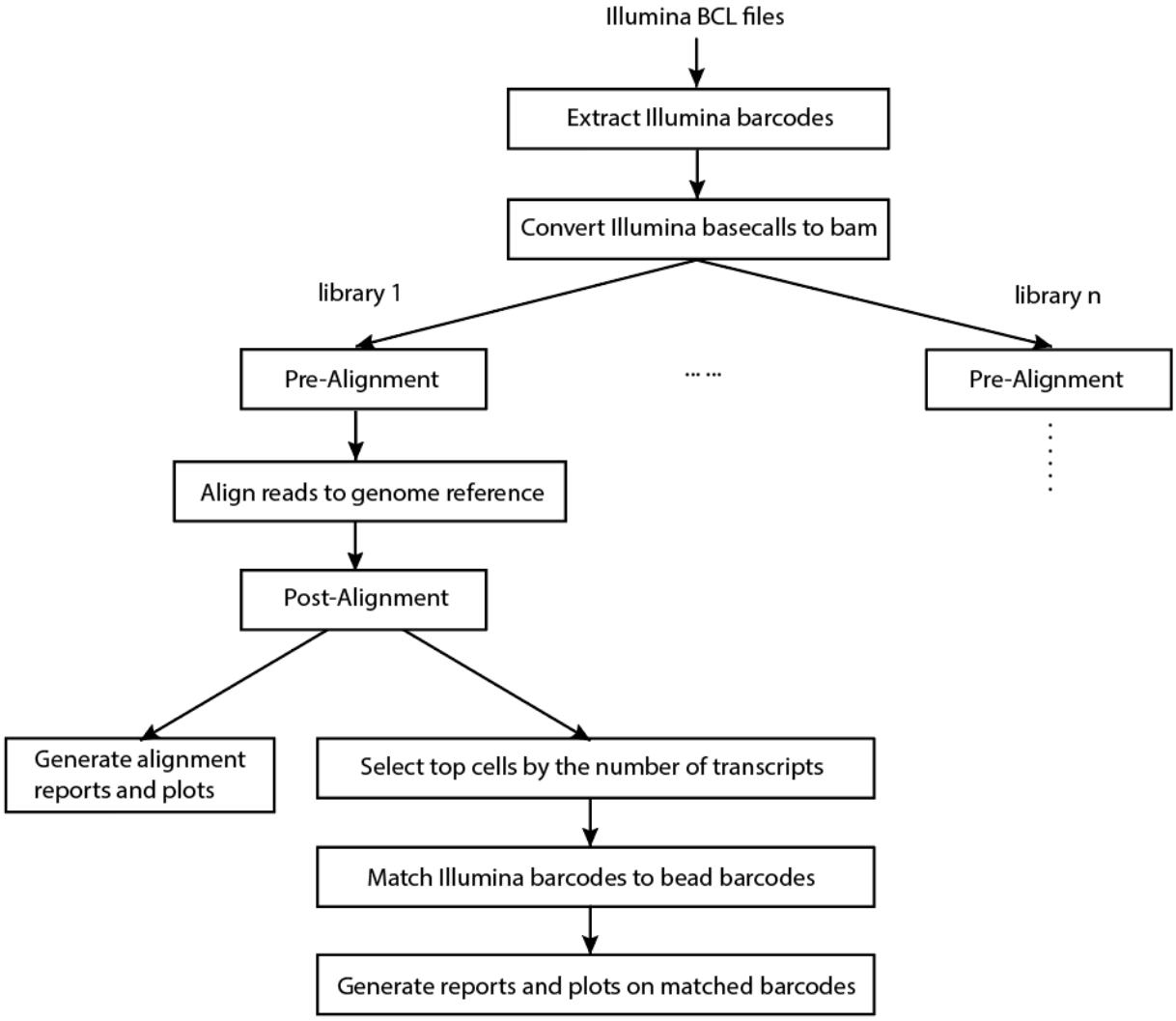

Figure S9: Workflow of the Slide-seq tools computational pipeline.

References

1. Codeluppi, S. *et al.* Spatial organization of the somatosensory cortex revealed by osmFISH. *Nat. Methods* **15**, 932–935 (2018).
2. Ainsley, J. A., Drane, L., Jacobs, J., Kittelberger, K. A. & Reijmers, L. G. Functionally diverse dendritic mRNAs rapidly associate with ribosomes following a novel experience. *Nat. Commun.* **5**, 4510 (2014).
3. Tushev, G. *et al.* Alternative 3’ UTRs Modify the Localization, Regulatory Potential, Stability, and Plasticity of mRNAs in Neuronal Compartments. *Neuron* **98**, 495–511.e6 (2018).